

Regular article

Stationary points on the H₂CO potential energy surface: dependence on theoretical level

Frank Jensen

Department of Chemistry, Odense University, DK-5230 Odense M., Denmark

Received: 5 February 1998 / Accepted: 21 May 1998 / Published online: 29 July 1998

Abstract. A total of 36 stationary points have been located on the H₂CO potential energy surface by means of gradient extremal following. These 36 points are believed to represent all the important stationary points on this surface. There is no indication that the structure of the surface becomes less complicated as the size of the basis set is enlarged at the Hartree-Fock level of theory, but many of the second- and third-order saddle points disappear when electron correlation is introduced. Of the ten first-order saddle points (transition structures) located, the majority have reaction paths entering the associated minima in a side-on approach, i.e. these cannot be located by uphill walking from the minimum.

Key words: Gradient extremal – Transition structure – Stationary points – H₂CO – Potential energy surface

1 Introduction

Transition structures (TS), which are first-order saddle points on a potential energy surface (PES), are important for understanding chemical reactions. Despite the existence of many different algorithms for locating such points, there are no general methods available which are guaranteed to find all TSs, or prove that a given TS does not exist. Most commonly used methods rely either on variations of the Newton-Raphson algorithm [1] or employ an interpolation scheme between the reactant and product [2].

With the recent development of a method for tracing gradient extremal (GE) curves it has become possible to locate essentially all stationary points on a given PES [3]. Although the method is computationally expensive, and therefore not suited for routine use, it allows complete mapping of low-dimensional surfaces, which can be used for testing the performance of less rigorous algorithms. In the present case we have investigated the H₂CO system, and located a total of 36 stationary points. At the Hartree-Fock (HF) level with the STO-3G, 3-21G and 6-31G(d,p) basis sets we have traced GEs to map out all

the important stationary points, which have been further refined at the complete active space self-consistent field (CASSCF) [4], second-order Møller-Plesset perturbation theory MP2 [5] and quadratic configuration interaction with singles and doubles (QCISD) [6] levels of theory. In addition to providing well-characterized reference systems, these results also allow us to examine two other questions:

- 1) How does the shape of a PES change as a function of the theoretical level (basis set and amount of electron correlation)?
- 2) What types of TSs exist on a “typical” PES calculated by electronic structure methods?

Answers to these questions may provide insight into the performance of existing algorithms for locating TSs, and possibly lead to the development of new algorithms.

2 Methods

An algorithm for tracing GEs has been described in detail previously [3]. For the present purpose it is sufficient to note that a GE is a one-dimensional curve consisting of points where the derivative of the gradient norm on an energy contour is zero. This is equivalent to the gradient being an eigenvector of the Hessian:

$$\begin{aligned} \frac{\partial |g|}{\partial x} = 0, \quad E(x) = \text{constant} \\ \Downarrow \\ Hg = \epsilon g \end{aligned}$$

This condition allows formulation of a predictor-corrector algorithm for tracing GEs [7]. A predictor step is taken along the tangent to the GE, followed by one or more corrector steps until the size of the correction drops below a selected threshold. The accuracy of the tracing is thus controlled by the cutoff for the correction step, while the sampling of the GE is controlled by the size of the predictor step. Each step (either predictor or corrector) requires two full Hessian calculations, making GE tracing computationally expensive.

At stationary points there are GEs leaving along all the normal modes. As a GE cannot vanish unless the gradient becomes zero, it will ultimately lead to one of three cases: a stationary point (which may or may not be different from the starting point), bond dissociation (the gradient goes asymptotically to zero), or the energy becomes very high due to atoms clashing. Scenarios two and three

are the normal behaviour when following GEs leaving along the highest modes, since these correspond to bond-stretching vibrations.

Starting from a given stationary point, all GEs leaving along the 3N-6 normal modes can be traced. This will lead to the discovery of new stationary points, which then can be subjected to GE tracing, etc. By using this procedure iteratively a large number of stationary points on a given surface can be located. Although it is possible to envision energy surfaces which have two (or more) sets of stationary points which are not connected by any GEs, our (limited) experience suggests that this is not the common behaviour. In practice, however, numerical problems may prevent a complete mapping. When the surface is very flat, for example, the Hessian has small eigenvalues which render the correction step numerically unstable. Or geometries may be encountered along the GE where it is difficult to achieve convergence of the wave function. An incomplete mapping may artificially lead to disconnected sets of stationary points, however, the present system is sufficiently small that we considered it unlikely that any important stationary points (i.e. not associated with loosely bound complexes) have been missed.

In the present case we traced all GEs radiating along normal modes with non-mass-weighted eigenvalues less than 0.2 a.u. for all stationary points [8]. This typically corresponds to the lowest three or four normal modes of the six available in H₂CO. At least 100 predictor steps of 0.10 a.u. were taken, and the correction step reduced below 10⁻³ a.u. In cases where GE bifurcations also crossing of two GEs) were encountered, the perpendicular GE was also followed. Each of the three surfaces, HF/STO-3G, HF/3-21G and HF/6-31G(d,p), was subjected to an exhaustive search, corresponding to approximately 45,000 Hessian calculations for each.

With a restricted Hartree-Fock (RHF) type wave function and the STO-3G, 3-21G and 6-31G(d,p) basis sets [5] we located all the important stationary points by tracing GEs as described above. The HF/6-31G(d,p) stationary points were refined with the larger cc-pVDZ and cc-pVTZ basis sets [9]. The HF/6-31G(d,p) stationary points were similarly subjected to re-optimizations at the [10, 12] CASSGF (full valence orbital space) and MP2/6-31G(d,p) levels [11]. For cases which did not readily converge at the MP2 level, electron correlation was gradually introduced by adding one orbital at a time. This presumably gives a good indication of whether the HF/6-31G(d,p) stationary points survive at the MP2 level, but there may be other stationary points at the MP2 level which we have missed. Performing a complete GE search at a correlated level is currently impractical.

The MP2/6-31G(d,p) stationary points were further refined by extending the basis sets to cc-pVDZ and cc-pVTZ. The sensitivity towards inclusion of more electron correlation was tested by re-optimizations at the QCISD/6-31G(d,p) level. For cases which did not readily optimize, we also performed optimizations at the MP3 and MP4(SDQ) levels prior to QCISD.

The nature of the TSs was established by tracing the intrinsic reaction coordinate (IRC) [12]. We note that many of the stationary points are energetically above the dissociation limit (say C + H₂O), however, for probing structural features of the PES, this is unimportant.

3 Results and discussion

There are four well-known minima on the H₂CO PES, corresponding to formaldehyde (MIN1), the H₂ + CO dissociation product (MIN2) and *trans*- and *cis*-hydroxycarbene (MIN3 and MIN4). We have located a fifth isomer, corresponding to an ylide-type structure, COH₂ (MIN5). Considering only structures which do not correspond to weakly bound complexes, we have located a total of 10 first-, 14 second- and 7 third-order saddle points [13]. Molecular plots are shown in Fig. 1, and Table 1 indicates at which levels of theory they exist and their relative energies. It can be noted that no saddle

►
Fig. 1. Stationary points on the H₂CO potential energy surface (PES). MIN minimum, TS transition structure (first-order saddle point), SOSP second-order saddle point, TOSP third-order saddle point. Distances in Å for HF/6-31G(d,p) optimized structures, except SOSP13, SOSP14 and TOSP7 which are HF/STO-3G values

points of higher order than three were found¹. This is consistent with the observation that minima 1, 3, 4 and 5 have three bonds, and thus $3 * 4 - 6 - 3 = 3$ remaining degrees of freedom. As energy maxima are not expected along coordinates corresponding to simple bond-length distortion, this suggests that saddle points should at most be at a maximum in three directions, as observed.

At the HF level of theory, all the minima and first-order saddle points in Table 1 are present with the STO-3G, 3-21G and 6-31G(d,p) basis sets. The only difference is that MIN5 has C_s symmetry with the STO-3G and 6-31G(d,p) basis sets (pyramidal oxygen), but C_{2v} with the 3-21G (planar oxygen). The existence of second- and third-order saddle points, however, depends on the size of the basis. The nature of the stationary point may also change, e.g. TOSP1 is a third-order saddle point with the STO-3G basis set, but a second-order saddle point with 3-21G and 6-31G(d,p). Similarly, TS13 and TS25 have C_s symmetry with 3-21G and 6-31G(d,p) basis sets, but these are second-order saddle points with the STO-3G basis, and there are consequently two symmetry equivalent C₁ structures which are first-order saddle points with this basis set. The C_s symmetric second-order saddle points are indicated in parentheses in Table 1. The use of basis sets larger than 6-31G(d,p) (cc-pVDZ and cc-pVTZ) gave only minor structural and energetic changes, except that TS24', SOSP12 and TOSP6 disappear as stationary points. The latter two points are very close in structure and energy, and are peculiar to the HF/6-31G(d,p) surface. In this structural region of space two different RHF solutions exist within a few kcal/mol of each other, both of which are minima in the orbital space. Although SOSP12 and TOSP6 are stationary points on the same energy surface (as evident from the atomic charges), the second close-lying solution apparently distorts the shape of the underlying surface.

When electron correlation is introduced (CASSCF, MP2 or QCISD), some of the TSs, and approximately half of the second- and third-order saddle points disappear. Since we have not traced GEs at the correlated level, there may be additional stationary points. If the geometries at the correlated levels are sufficiently different from those at HF/6-31G(d,p), the optimization may fail to converge. Extending the basis set to cc-pVDZ and cc-pVTZ at the MP2 level did not change the conclusions obtained with the 6-31G(d,p), but the stationary points corresponding to TS24' and TS25 apparently do not exist at the QCISD level, i.e. these are sensitive to inclusion of additional electron correlation. It can also

¹Test calculations with the STO-3G basis set indicate that this is not the result of only following GEs radiating along the lowest three or four modes

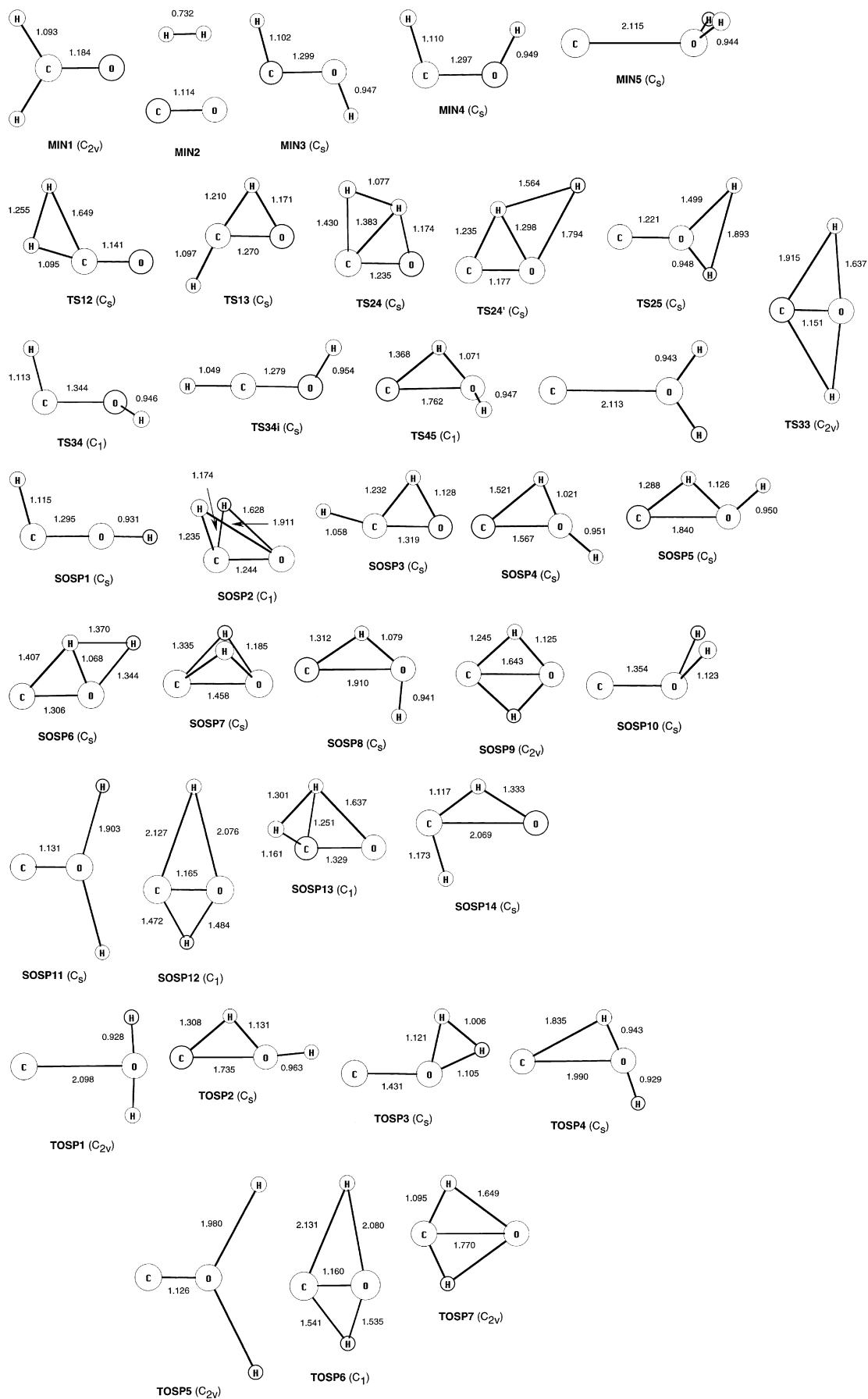


Table 1. Stationary points as a function of level of theory. Energies in kcal/mol. RHF restricted Hartree-Fock, CASSCF complete active space self-consistent field, MP2 second-order Møller-Plesset perturbation theory, QCISD quadratic configuration interaction with singles and doubles

	RHF STO-3G	RHF 3-21G	RHF 6-31G(d,p)	CASSCF 6-31G(d,p)	MP2 6-31G(d,p)	QCISD 6-31G(d,p)
MIN1	0	0	0	0	0	0
MIN2	7	3	0	-14	3	3
MIN3	48	47	49	61	59	54
MIN4	53	54	55	55	64	59
MIN5	173	135	156	160	178	168
TS12	141	108	105	85	95	94
TS13	119 (128) ^a	108	101	91	90	91
TS24	158	137	124	115	116	115
TS24'	265	233	219		194	
TS25	239 (251) ^a	190	192		165 (MIN)	
TS33	280	218	214			
TS34	77	74	77	81	91	85
TS34i	130	115	122	122	131	127
TS45	193	159	172	169	183	172
TS55	174	(MIN5)	156	161	(MIN5)	169
SOSP1	97	78	86	88	97	92
SOSP2	178		162	151	153	150
SOSP3	201	175	169	157	159	157
SOSP4	209	163	181	180	191	182
SOSP5	210		182	182	195	183
SOSP6	266	235	231	209	217	205
SOSP7			226	209	207	207 (TS)
SOSP8	213	167	178	175		
SOSP9	230	196	195	180		
SOSP10	241	209	221	183		
SOSP11		231	228			
SOSP12			233			
SOSP13	177					
SOSP14	203					
TOSP1	242	170 (SOSP)	188 (SOSP)	193	209	200
TOSP2	218		185	184	196	186
TOSP3	269	235	240		240	212
TOSP4		171	188	193		
TOSP5		234	231			
TOSP6			233			
TOSP7	215					

^a C_s Symmetric second-order saddle points

be noted that TOSP1 returns to being a third-order saddle point at correlated levels, although it is a second-order saddle point at the HF/3-21G and HF/6-31G(d,p) levels. Finally, SOSP7 becomes a TS connecting MIN2 with a complex corresponding to H₂O + C at the QCISD level.

Although it is commonly believed that a PES is more “knobby” with a minimum basis set (as the STO-3G) than a larger DZP type [as the 6-31G(d,p)], this is apparently not the case for the present system. The data may indicate, however, that the PES is smoother at correlated levels, since there is a substantially smaller number of second- and third-order saddle points.

The HF/6-31G(d,p) relative energies and connectivity between minima and TSs are shown in Fig. 2. There are two important conclusions which can be drawn from the present data, and which are likely to remain true also for more complicated systems:

- 1) There is not necessarily a TS connecting all pairs of minima. For example, there is no direct path between formaldehyde (MIN1) and *cis*-hydroxycarbene (MIN4).
- 2) There may be more than one TS connecting two pairs of minima. For example, there is both a

rotation² (TS34) and inversion (TS34i) pathway between the *trans*- and *cis*-hydroxycarbene, and two distinct ways of dissociating *cis*-hydroxycarbene to H₂ + CO (TS24 and TS24'). The two different modes of interconversion of the *trans*- and *cis*-hydroxycarbene are analogous to the situation in the isoelectronic diazene (N₂H₂) molecule [14].

Operationally the TSs can be placed into two groups: those which can be located by “walking” up a Hessian mode starting directly from a minimum [15], and those which require a starting geometry in the (close) vicinity of the TS for Newton-Raphson methods to work. Conceptually these may be associated with an “end of a valley” type TS (type a, Fig. 3) and a “side-on” TS (type b, Fig. 3). The “end of a valley” type TSs are marked with bold lines in Fig. 2. It is clear that the majority of the TSs are of the “side-on” type b, which are much harder to locate by Newton-Raphson optimization routines.

Cases corresponding to type a are expected to have IRCs which are relatively straight, while IRCs belonging to type b are expected to be strongly curved in some

²Note that TS34 is a rotation of the OH group, and not the CH group, since the oxygen inversion corresponds to SOSP1, while the carbon inversion is a TS (TS34i)

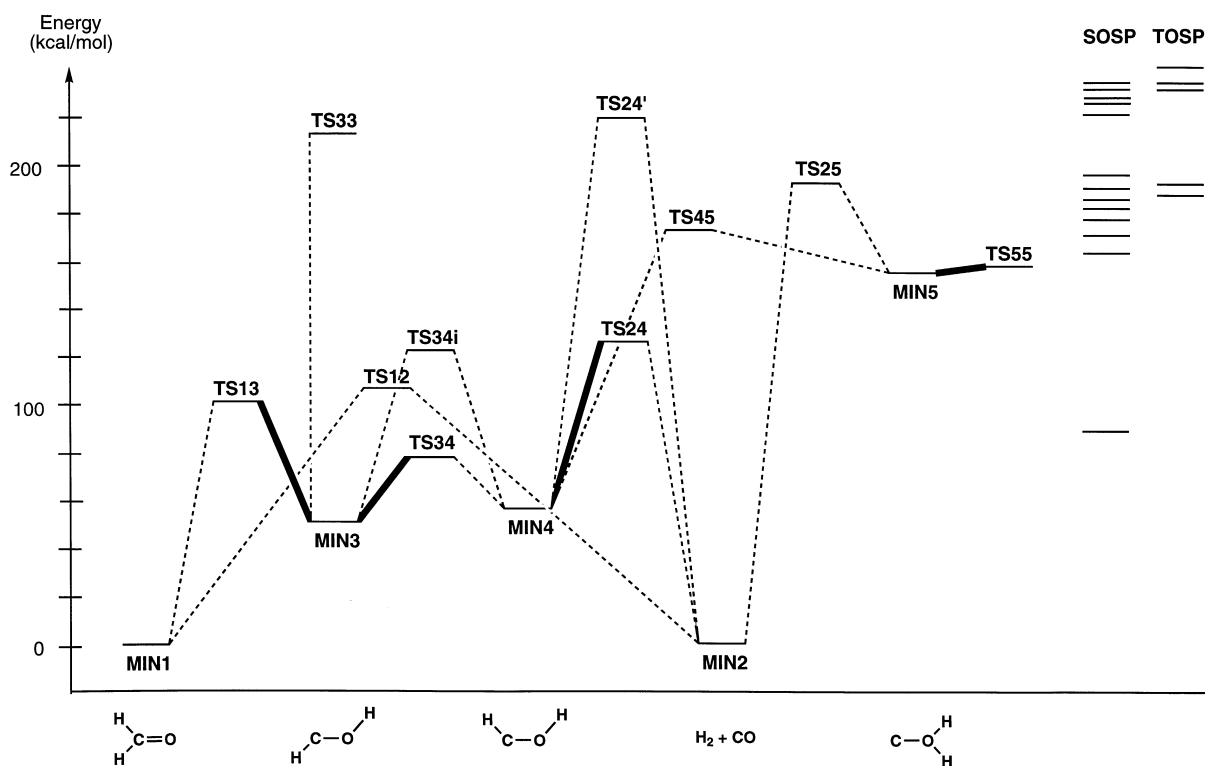


Fig. 2. Relative energies of stationary points on the H_2CO PES at the HF/6-31G(d,p) level. Bold lines indicate TSs which can be located by mode following from the corresponding minimum

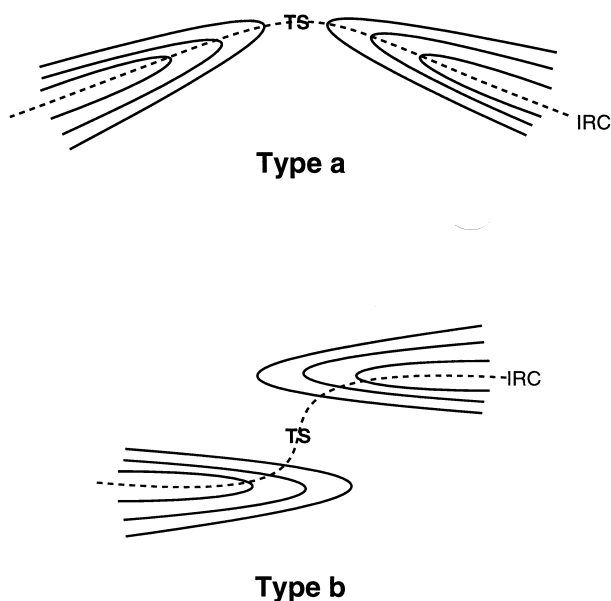


Fig. 3a, b Illustration of: **a** an “end of the valley” type TS and **b** “side-on” type TS

region of the IRC. The curvature k of an IRC can be calculated from the gradient and Hessian as

$$k = (I - tt^\dagger)Ht/|g|$$

where t is the normalized gradient vector [16]. Inspection of the curvature along the IRC paths, however, did not

reveal an obvious correlation between the magnitude of the curvature and which TSs can be located by uphill walking from the minimum. There is a trend that IRCs associated with TSs of type a have smaller curvature, but this is not uniformly true.

TS34, which corresponds to a simple bond rotation, is a good example of how subtle differences can determine whether a reaction path belongs to type a or b. The path connecting TS34 with MIN3 is of type a, and is in fact the only case where the IRC closely follows the corresponding GE. The path connecting TS34 with MIN4 is in contrast of type b. The difference is due to a switching of the two lowest Hessian modes for MIN3 and MIN4, both of which have C_s symmetry. In MIN4 the lowest mode is symmetric (a'), while the lowest mode in MIN3 is asymmetric (a''). Since TS34 has no symmetry, it is clear that only from MIN3 can the TS be reached by climbing the lowest mode. For MIN4 the second lowest mode (of a'' symmetry) must be followed initially, but since it must end up as the lowest mode at the TS, the lowest and second lowest modes must cross at some point (degenerate eigenvalues in the Hessian). In this region an uphill walk becomes unguided [15]. An alternative way of viewing the situation is that the IRC always enters a minimum along the lowest Hessian mode of the given symmetry [17]. Since TS34 has no symmetry, the IRC will enter both MIN3 and MIN4 along the lowest mode. For MIN4 this means that the IRC will enter the minimum asymptotically along a symmetric direction, as the lowest mode is symmetric, and it is consequently not possible to reach the TS by uphill walking.

The fact that the IRC always enters a minimum along the lowest mode of a given symmetry means that for a minimum belonging to an Abelian point group having R

different irreducible representations, there can at most be $R + 1$ TSs of type a (Fig. 3). Furthermore, this can only be the case if the lowest mode is totally symmetric, in other cases there will at maximum be $R - 1$. For a non-symmetric C_1 molecule there are thus at most two TSs which can be reached by mode following, for point groups C_2 , C_s and C_i there may be either three or one TSs, depending on whether the lowest mode is totally symmetric or not. It should be noted, however, mode that which mode that has the lowest eigenvalue can be changed for example by mass-weighting of the atoms.

4 Conclusions

By using GE following we have located all the important stationary points on the H_2CO PES at the HF level of theory with the STO-3G, 3-21G and 6-31G(d,p) basis sets. A substantial number of the second- and third-order saddle points disappears when electron correlation is introduced, indicating that the energy surface is smoother when correlation is included. Analysis of the intrinsic reaction paths for the first-order saddle points show that most of the TSs are located on the side of the valley on the surface, and can therefore not be located by uphill walking from the energy minimum.

Acknowledgements This work was supported by grants from the Danish Natural Science Research Council.

References

- (a) Fletcher R (1987) Practical methods of optimizations. Wiley, New York; (b) Banerjee A, Adams N, Simons J, Shepard R (1985) *J Phys Chem* 89:52; (c) Helgaker T (1991) *Chem Phys Lett* 182:503; (d) Culot P, Dive G, Nguyen VH, Ghuysen JM (1992) *Theor Chim Acta* 82: 189; (e) Schlegel HB (1987) *Adv Chem Phys* 67:249; (f) Schlegel HB (1995) In: Yarkony DR (ed) *Modern electronic structure Theory*:p 459 World Scientific
- (a) Dewar MJS, Healy EF, Stewart JJP (1984) *J Chem Soc Faraday Trans 2* 80:227 (b) Czerninski R, Elber R (1990) *Int J Quantum Chem Symp* 24:167; (c) Choi C, Elber RJ (1991) *Chem Phys* 94:751; (d) Liotard DA (1992) *Int J Quantum Chem* 44:723; (e) Fischer T, Karplus M (1992) *Chem Phys Lett* 194:252; (f) Peng C, Schlegel HB (1993) *Isr J Chem* 33:449; (g) Ionova IV, Carter EA (1995) *J Chem Phys* 103:5437; (h) Cardenas-Lailhacar C, Zerner MC (1995) *Int J Quantum Chem* 55:429; (i) Ayala PY, Schlegel HB (1997) *J Chem Phys* 107:375
- Bondensgaard K, Jensen F (1996) *J Chem Phys* 104:8025
- Roos BO (1987) *Adv Chem Phys* 69:399
- Hehre WJ, Radom L, Schleyer PvR, Pople JA (1986) *Ab initio molecular orbital theory*. Wiley, New York
- Pople JA, Head-Gordon M, Raghavachari K (1987) *J Chem Phys* 87:5968
- Sun J, Ruedenberg K (1993) *J Chem Phys* 98:9707
- GAMESS-US: Schmidt MW, Baldrige KK, Boatz JA, Elbert ST, Gordon MS, Jensen JH, Koseki S, Matsunaga N, Nguyen KA, Su SJ, Windus TL, Dupuis M, Montgomery JA (1993) *J Comput Chem* 14: 1347
- Dunning TH Jr (1989) *J Chem Phys* 90:1007
- DALTON 1.0: Helgaker T, Jensen HJA, Jørgensen P, Olsen J, Ruud K, Ågren H, Andersen T, Bak KL, Bakken V, Christiansen O, Dahle P, Dalskov EK, Enevoldsen T, Fernandez B, Heiberg H, Hetttema H, Jonsson D, Kirpekar S, Kobayashi R, Koch H, Mikkelsen KV, Norman P, Packer MJ, Saue T, Taylor PR, Vahtras O (1997)
- Gaussian 94: Frisch MJ, Trucks GW, Schlegel HB, Gill PMW, Johnson BG, Robb MA, Cheeseman JR, Keith T, Petersson GA, Montgomery JA, Raghavachari K, Al-Laham MA, Zakrzewski VG, Ortiz JV, Foresman JB, Cioslowski, J, Stefanov BB, Nanayakkara A, Challacombe M, Peng CY, Ayala PY, Chen W, Wong MW, Andres JL, Replogle ES, Gomperts R, Martin RL, Fox DJ, Binkley JS, Defrees DJ, Baker J, Stewart JJP, Head-Gordon M, Gonzalez C, Pople JA (1995) Gaussian, Inc., Pittsburgh Pa.
- Fukui K (1981) *Acc Chem Res* 14:363
- All geometries can be obtained from the author by e-mail request: frj@dou.dk
- Jensen HJA, Jørgensen P, Helgaker T (1987) *J Am Chem Soc* 109:2895
- Jensen F (1995) *J Chem Phys* 102:6706
- Sun JQ, Ruedenberg K (1993) *J Chem Phys* 99:5257
- Tachibana A, Fukui K (1979) *Theor Chim Acta* 51:189